PHYSICAL REVIEW D **81,** 044022 (2010)

Test particle motion around a black hole in a braneworld

Ahmadjon Abdujabbarov* and Bobomurat Ahmedov†

Institute of Nuclear Physics, Ulughbek, Tashkent 100214, Uzbekistan, Ulugh Beg Astronomical Institute, Astronomicheskaya 33, Tashkent 100052, Uzbekistan, Inter University Centre for Astronomy & Astrophysics, Post Bag 4, Pune 411007, India

(Received 23 January 2009; revised manuscript received 22 January 2010; published 12 February 2010)

Analytical solutions of Maxwell equations in background spacetime of a black hole in a braneworld immersed in an external uniform magnetic field have been found. The influence of both magnetic and brane parameters on the effective potential of the radial motion of a charged test particle around a slowly rotating black hole in a braneworld immersed in a uniform magnetic field has been investigated by using the Hamilton-Jacobi method. An exact analytical solution for dependence of the radius of the innermost stable circular orbits (ISCO) $r_{\rm ISCO}$ from the brane parameter for the motion of a test particle around a nonrotating isolated black hole in a braneworld has been derived. It has been shown that the radius $r_{\rm ISCO}$ is monotonically growing with the increase of the module of the brane tidal charge. A comparison of the predictions on $r_{\rm ISCO}$ of the braneworld model and of the observational results of ISCO from relativistic accretion disks around black holes provided the upper limit for the brane tidal charge $\lesssim 10^9$ cm^2.

DOI: 10.1103/PhysRevD.81.044022 PACS numbers: 04.50.−h, 04.40.Dg, 97.60.Gb

I. INTRODUCTION

The idea that our Universe might be a three-brane [1], embedded in a higher dimensional spacetime, has recently attracted much attention. For astrophysical interests, static and spherically symmetric exterior vacuum solutions of the braneworld models were initially proposed by Dadhich *et al.* [2,3] which have the mathematical form of the Reissner-Nordström solution, in which a tidal Weyl parameter Q^* plays the role of the electric charge squared of the general relativistic solution. The so-called Dadhich-Maartens-Papodopoulos-Rezania (DMPR) solution was obtained by imposing the null energy condition on the three-brane for a bulk having a nonzero Weyl curvature.

Observational possibilities of testing the braneworld black hole models at an astrophysical scale have been intensively discussed in the literature during the last several years, for example, through the gravitational lensing [4–9], the motion of test particles [10], and the classical tests of general relativity (perihelion precession, deflection of light, and the radar echo delay) in the Solar System [11]. The role of the tidal charge in orbital models of high-frequency quasiperiodic oscillations observed in neutron star binary systems has been also studied [12]. In paper [13] the energy flux, the emission spectrum, and accretion efficiency from the accretion disks around several classes of static and rotating braneworld black holes have been obtained. The complete set of analytical solutions of the geodesic equation of massive test particles in higher dimensional spacetimes which can be applied to braneworld models is provided in the recent paper [14]. Recently the deflection angle of light rays caused by a massive black hole in a braneworld in the weak lensing approach has been derived, up to the second order in perturbation theory [15,16]. The influence of the tidal charge onto profiled spectral lines generated by radiating tori orbiting in the vicinity of a rotating black hole has been studied in paper [17]. Authors showed that with lowering the negative tidal charge of the black hole, the profiled line becomes flatter and wider, keeping their standard character with flux stronger at the blue edge of the profiled line. The role of the tidal charge in the orbital resonance model of quasi-periodic oscillations in black hole systems has been investigated in paper [18]. The influence of the tidal charge parameter of the braneworld models on some optical phenomena in rotating black hole spacetimes has been extensively studied in paper [19].

A braneworld corrections to the charged rotating black holes and to the perturbations in the electromagnetic potential around black holes are studied in [20,21]. Our preceding paper [22] was devoted to the stellar magnetic field configurations of relativistic stars in dependence on brane tension. Here we plan to study electromagnetic fields and particle motion around a rotating black hole in a braneworld immersed in a uniform magnetic field. The study of the particle orbits could provide an opportunity for constraining the allowed parameter space of solutions, and to provide a deeper insight into the physical nature and properties of the corresponding spacetime metrics. Therefore, this may open up the possibility of testing braneworld models by using astronomical and astrophysical observations around black holes, in particular, observationally measured ISCO radii around black holes in principle may give definite constraints on the numerical value of the brane tidal charge. The motion of test particles near black holes immersed in an asymptotically uniform magnetic field and some gravity surrounding structure, which provides the magnetic field has been intensively studied in paper [23]. The author has calculated the binding

*ahmadjon@astrin.uzsci.net
†ahmedov@astrin.uzsci.net

energy for spinning particles on circular orbits. The bound states of the massive scalar field around a rotating black hole immersed in the asymptotically uniform magnetic field is considered in paper [24].

The paper is organized as follows. In Sec. II we look for exact solutions of vacuum Maxwell equations in the spacetime of the rotating black hole in a braneworld immersed in a uniform magnetic field. In Sec. III the motion of charged particles around a black hole in a braneworld immersed in a uniform magnetic field has been studied in the slow rotation approximation. We obtain the effective potential for any particle with a specific angular momentum, orbiting around the black hole, as a function of the magnetic field, and of the tidal charge of the black hole. The exact expression for the dependence of the radius of an innermost stable circular orbit from the brane charge has been found in Sec. IV for the test particle moving in the equatorial plane of the black hole in a braneworld when both rotation and magnetic parameters are neglected for the simplicity of calculations. Then we present a clear derivation of the capture cross section of slowly moving test particles by a black hole in a braneworld. The exact expressions for the critical angular momentum of the test particle and corresponding radius of unstable circular orbits of the particle around the black hole have been presented. For different tidal charges, the values of the radii of the marginally stable orbits around a black hole in a braneworld are also plotted. The conclusion and discussion of the obtained results can be found in Sec. V.

We use in this paper a system of units in which $c = 1$, a spacelike signature $(-, +, +, +)$, and a spherical coordinate system (t, r, θ, φ). Greek indices are taken to run from 0 to 3, Latin indices from 1 to 3, and we adopt the standard convention for the summation over repeated indices. We will indicate vectors with bold symbols (e.g. $\boldsymbol{B}$).

II. ROTATING BLACK HOLE IN A BRANEWORLD IMMERSED IN A UNIFORM MAGNETIC FIELD

The spacetime metric of the rotating black hole in a braneworld in coordinates t, r, θ, φ takes the form (see e.g, [20])

$$\begin{aligned} ds^2 = &-\frac{\Delta - a^2\sin^2\theta}{\Sigma}dt^2 \\ &+ \frac{(\Sigma + a^2\sin^2\theta)^2 - \Delta a^2\sin^2\theta}{\Sigma}\sin^2\theta d\varphi^2 + \frac{\Sigma}{\Delta}dr^2 \\ &+ \Sigma d\theta^2 - 2\frac{\Sigma + a^2\sin^2\theta - \Delta}{\Sigma}a\sin^2\theta d\varphi dt, \end{aligned} \tag{1}$$

where $\Sigma = r^2 + a^2\cos^2\theta$, $\Delta = r^2 + a^2 - 2Mr + Q^*$, Q^* is the bulk tidal charge, M is the total mass, and a is related to the angular momentum of the black hole.

It is not difficult to show that the electromagnetic corrections created by the external magnetic field being proportional to the electromagnetic energy density are rather small for black holes. Indeed if B is the external magnetic field around a black hole in a braneworld of total mass M at radius r, these corrections are at most

$$\frac{B^2r^3}{8\pi Mc^2} \simeq 2.5\times 10^{-3}\left(\frac{B}{10^3\,\mathrm{G}}\right)^2\left(\frac{3\cdot M_{\odot}}{M}\right)\left(\frac{r}{1.5\,\mathrm{km}}\right)^3. \tag{2}$$

A Killing vector ξ^μ being an infinitesimal generator of an isometry satisfies to the equation

$$\xi_{\alpha;\beta} + \xi_{\beta;\alpha} = 0, \tag{3}$$

which can be used in order to rewrite the equation

$$\xi_{\alpha;\beta;\gamma} - \xi_{\alpha;\gamma;\beta} = -\xi^\lambda R_{\lambda\alpha\beta\gamma}, \tag{4}$$

which defines the Riemann curvature tensor $R_{\lambda\alpha\beta\gamma}$ in the form

$$\xi^{\alpha;\beta}{}_{;\beta} = \xi^\gamma R_{\gamma\beta}{}^{\alpha\beta} = R^\alpha{}_\gamma\xi^\gamma. \tag{5}$$

For the spacetime of the rotating black hole in the braneworld the right-hand side of Eq. (5) can be expressed as $R^\alpha{}_\gamma\xi^\gamma = \eta^\alpha$ and consequently the Maxwell equations as

$$F^{\alpha\beta}{}_{;\beta} = -2\xi^{\alpha;\beta}{}_{;\beta} + 2\eta^\alpha = 0, \tag{6}$$

where $\eta^\alpha = \{Q^*/M, 0, 0, 0\}$ (see [13,20,25]) and the electromagnetic field tensor $F_{\alpha\beta}$ can be selected as

$$\begin{aligned} F_{\alpha\beta} &= C_0(\xi_{\beta;\alpha} - \xi_{\alpha;\beta}) + f_{\alpha\beta} \\ &= -2C_0(\xi_{\alpha;\beta}) + a_{\beta,\alpha} - a_{\alpha,\beta}. \end{aligned} \tag{7}$$

Here C_0 is constant and 4-potential a^α being responsible for the tidal charge can be found from the equation $\Box a^\alpha = \eta^\alpha$.

Finally, one can express the electromagnetic potential as a sum of two contributions

$$A^\alpha = \tilde{A}^\alpha + a^\alpha. \tag{8}$$

where $\tilde{A}^\alpha$ is the potential being proportional to the Killing vectors. To find the solution for $\tilde{A}^\alpha$ we exploit the existence in this spacetime of a timelike Killing vector $\xi^\alpha_{(t)}$ and spacelike one $\xi^\alpha_{(\varphi)}$ being responsible for stationarity and the axial symmetry of geometry, such that they satisfy the Killing equations (3) and consequently the wavelike equations (in vacuum spacetime) $\Box\xi^\alpha = 0$, which gives a right to write the solution of vacuum Maxwell equations $\Box\tilde{A}^\alpha = 0$ for the vector potential $\tilde{A}_\alpha$ of the electromagnetic field in the Lorentz gauge in the simple form $\tilde{A}^\alpha = C_1 \xi^\alpha_{(t)} + C_2 \xi^\alpha_{(\varphi)}$ [26]. The constant $C_2 = B/2$, where the gravitational source is immersed in the uniform magnetic field **B** being parallel to its axis of rotation. The value of the remaining constant $C_1 = aB$ can be easily calculated from the asymptotic properties of spacetime (1) at the infinity (see e.g. our preceding paper [27] for the details of typical calculations).

The second part a^α of the total vector potential of the electromagnetic field is produced by the presence of the tidal charge and has the following solution: $a^\alpha = \{kQ^*/r, 0, 0, 0\}$, where expression for the constant $k = \pi aB/6M^2$ can be easily found from the asymptotic properties of spacetime (1) at the infinity [27].

Finally the components of the 4-vector potential A_α of the electromagnetic field will take a form

$$\begin{aligned} A_0 &= \frac{aB}{2\Sigma}[(2-\sin^2\theta)(a^2\sin^2\theta - \Delta) - \Sigma\sin^2\theta] \\ &\quad - \left(1 - \frac{2Mr - Q^*}{\Sigma}\right)\frac{kQ^*}{r}, \\ A_1 &= A_2 = 0, \\ A_3 &= \frac{B\sin^2\theta}{2\Sigma}[(\Delta - \Sigma - a^2)(2-\sin^2\theta)a^2 \\ &\quad + \Sigma(\Sigma + \sin^2\theta)] - \frac{2Mr - Q^*}{\Sigma}\frac{kQ^*}{r}a\sin^2\theta. \end{aligned} \tag{9}$$

The nonvanishing orthonormal components of the electromagnetic fields measured by zero angular momentum observers (ZAMO) with the four-velocity components

$$\begin{aligned} (u^\alpha)_{\rm ZAMO} &\equiv \frac{K}{\sqrt{\Delta\Sigma}}\left(1, 0, 0, \frac{a^2\sin^2\theta}{\Delta - a^2\sin^2\theta} - 1\right), \\ (u_\alpha)_{\rm ZAMO} &\equiv \frac{\sqrt{\Delta\Sigma}}{K}(1, 0, 0, 0), \end{aligned} \tag{10}$$

are given by expressions

$$\begin{aligned} E^{\hat r} &= \frac{aB}{\Sigma^2}\Bigg\{2(M-r) + M\sin^2\theta + \frac{\sin^4\theta}{\Delta - a^2\sin^2\theta}(\Sigma - \Delta + a^2\sin^2\theta)\left[r\Sigma + a^2(2-\sin^2\theta)\frac{r\Delta - a^2 r + (M-r)\Sigma}{\Sigma}\right] \\ &\quad + \frac{r}{\Sigma}(2-\sin^2\theta)[\Sigma^2 + (\Delta - a^2\sin^2\theta)(2-\sin^2\theta)]\Bigg\}K \\ &\quad - \frac{kQ^* a\sin^2\theta}{\Sigma^3 r^2}\left[4Q^* r^2 - 8Mr^3 - \Sigma^2 + \frac{4Mr^3 - Q^*\Sigma - 2Q^* r^2}{\Delta - a^2\sin^2\theta}a^2\sin^2\theta\right]K, \end{aligned} \tag{11}$$

$$\begin{aligned} E^{\hat\theta} &= \frac{aB\sin 2\theta}{2\Sigma^2\sqrt{\Delta}}\Bigg\{a^2\sin^2\theta - \Delta - \Sigma + \frac{a^2\sin^2\theta - \Delta + \Sigma}{\Sigma}a^2(2-\sin^2\theta) + \frac{a^2\sin^2\theta - \Delta + \Sigma}{\Delta\csc^2\theta - a^2} \\ &\quad \times\left[(\Sigma + a^2(2+\cos^2\theta) - \Delta)a^2\sin^2\theta + \Sigma(\Sigma + a^2\sin^2\theta) - \frac{\Sigma - \Delta + a^2}{\Sigma}a^2(\Sigma + a^2\sin^2\theta)(2-\sin^2\theta)\right]\Bigg\}K \\ &\quad + \frac{kQ^* a\sin 2\theta}{r\Sigma\sqrt{\Delta}}\left[\frac{2Mr - Q^*}{\Sigma}\frac{r^2+a^2}{\Sigma}\frac{a\sin^2\theta}{\Delta - a^2\sin^2\theta} - 1\right]K, \end{aligned} \tag{12}$$

$$\begin{aligned} B^{\hat r} &= \frac{B\csc\theta}{2K\Sigma}[(\Sigma + a^2(2+\cos^2\theta) - \Delta)a^2\sin^2\theta \\ &\quad + \Sigma(\Sigma + a^2\sin^2\theta) - \frac{\Sigma - \Delta + a^2}{\Sigma}a^2(\Sigma + a^2\sin^2\theta) \\ &\quad \times(2-\sin^2\theta)\Big] + \frac{2Mr - Q^*}{\Sigma}\frac{r^2+a^2}{Kr}kQ^* a\sin^2\theta, \end{aligned} \tag{13}$$

$$\begin{aligned} B^{\hat\theta} &= \frac{B\sin\theta\sqrt{\Delta}}{K\Sigma}\Bigg[r\Sigma + a^2(2-\sin^2\theta) \\ &\quad \times\frac{r\Delta - a^2 r + (M-r)\Sigma}{\Sigma}\Bigg] + \frac{\sqrt{\Delta}}{K} \\ &\quad \times\frac{Q^*\Sigma + 4Mr^3 - 2Q^* r^2}{r^2\Sigma}kQ^* a\sin^2\theta, \end{aligned} \tag{14}$$

which depend on the angular momentum and tidal charge in a complex way and where we have used $K = ((\Sigma + a^2\sin^2\theta)^2 - a^2\Delta\sin^2\theta)^{1/2}$. In the limit of flat spacetime, i.e. for $M/r \to 0$, $Ma/r^2 \to 0$, and $Q^*/r^2 \to 0$, expressions (11)–(14) give the following limiting expressions: $B^{\hat r} = B\cos\theta$, $B^{\hat\theta} = B\sin\theta$, $E^{\hat r} = E^{\hat\theta} = 0$, which coincide with the solutions for the homogeneous magnetic field in Newtonian spacetime. Here ^ (hat) stands for the orthonormal components of the electric and magnetic fields. The uniform magnetic field in the background of a five dimensional black hole has been extensively studied in [28]. In particular, authors presented exact expressions for two forms of an electromagnetic tensor and the electrostatic potential difference between the event horizon of a five dimensional black hole and the infinity.

III. CHARGED PARTICLE MOTION IN THE VICINITY OF A ROTATING BLACK HOLE IN A BRANEWORLD

In this section we investigate in detail the motion of charged particles around a rotating black hole in a braneworld in an external magnetic field given by a 4-vector potential (9) with the aim to find a way for astrophysical evidence for either the existence or nonexistence of a tidal charge Q^*. For simplicity of calculations we assume parameter a to be small, and obtain the exterior metric for a slowly rotating compact object in the braneworld in the following form:

$$ds^2 = -A^2dt^2 + H^2dr^2 + r^2d\theta^2 + r^2\sin^2\theta d\varphi^2 - 2\tilde{\omega}(r)r^2\sin^2\theta dt d\varphi, \quad (15)$$

here

$$A^2(r) \equiv \left(1 - \frac{2M}{r} + \frac{Q^*}{r^2}\right) = H^{-2}(r), \quad (16)$$

is the corresponding metric function of the tidal charged compact object of the solution [2] for the metric outside the gravitating object and $\tilde{\omega}(r) = \omega(1 - Q^*/2rM) = 2Ma/r^3(1 - Q^*/2rM)$.

The Hamilton-Jacobi equation

$$g^{\mu\nu}\left(\frac{\partial S}{\partial x^\mu} + eA_\mu\right)\left(\frac{\partial S}{\partial x^\nu} + eA_\nu\right) = -m^2, \quad (17)$$

for the motion of the charged test particles with mass m and charge e is applicable as a useful computational tool only when the separation of variables can be effected.

Since the spacetime of the rotating object in a braneworld admits such separation of variables (see e.g. [29]) we shall study the motion around the source described with metric (15) using the Hamilton-Jacobi equation when the action S can be decomposed in the form

$$S = -\mathcal{E}t + \mathcal{L}\varphi + S_{r\theta}(r, \theta), \quad (18)$$

since the energy $\mathcal{E}$ and the angular momentum $\mathcal{L}$ of a test particle are constants of motion in the spacetime (15).

Therefore the Hamilton-Jacobi equation (17) with action (18) implies the equation for the inseparable part of the action as

$$\begin{aligned}\frac{1}{2A^2}\bigg[&\mathcal{E} + \frac{a}{r}\left(\frac{2M\mathcal{L}}{r^2} - \frac{Q^*\mathcal{L}}{r^3} + A^2eB + A^2ek\frac{Q^*}{r}\right)\bigg] \\ &\times\left[2\mathcal{E} + aeBA^2 + A^2ek\frac{Q^*}{r} - aeB\left(\frac{2M}{r} - \frac{Q^*}{r^2}\right)\sin^2\theta\right] \\ &+ \left(\mathcal{L} + \frac{1}{2}eBr^2\sin^2\theta\right)\bigg[\frac{eB}{2} + A^2ek\frac{Q^*}{r} + \frac{\mathcal{L}}{r^2\sin^2\theta} \\ &- \frac{a\mathcal{E}}{r^2A^2}\left(\frac{2M}{r} - \frac{Q^*}{r^2}\right)\bigg] + A^2\left(\frac{\partial S_{r\theta}}{\partial r}\right)^2 + \frac{1}{r^2}\left(\frac{\partial S_{r\theta}}{\partial \theta}\right)^2 = -m^2.\end{aligned} \quad (19)$$

It is not possible to separate variables in this equation in the general case but it can be done for the motion in the equatorial plane $\theta = \pi/2$ when the equation for radial motion takes the form

$$\left(\frac{dr}{d\sigma}\right)^2 = \mathcal{E}^2 - 1 - 2V_{\rm eff}(\mathcal{E}, \mathcal{L}, r, \epsilon, a, Q^*). \quad (20)$$

Here σ is the proper time along the trajectory of a particle, $\mathcal{E}$ and $\mathcal{L}$ are energy and angular momentum per unit mass m, and

$$\begin{aligned}V_{\rm eff}(\mathcal{E}, \mathcal{L}, r, \epsilon, a, Q^*) = &\frac{a\mathcal{E}\mathcal{L}}{r^2}\left(\frac{2M}{r} - \frac{Q^*}{r^2}\right) \\ &+ \left(\frac{\mathcal{L}^2}{2r^2} + \frac{\epsilon\mathcal{L}}{2} + \frac{\epsilon^2r^2}{8} + a\mathcal{E}\epsilon \right. \\ &\left. + \frac{\pi Q^* a\epsilon}{M^2r}\right)A^2 - \frac{M}{r} + \frac{Q^*}{2r^2}\end{aligned} \quad (21)$$

is the effective potential, where $\epsilon = eB/m$ is the magnetic parameter.

Figure 1 shows the radial dependence of the effective potential of the radial motion of a charged particle on an equatorial plane of a slowly rotating black hole in a braneworld immersed in a uniform magnetic field for different values of the parameter of the magnetic field (left graph) and tidal charge (right one). One can obtain now how magnetic and brane parameters change the character of the motion of the charged particle. Both magnetic and tidal parameters are responsible for shifting the shape of the effective potential to the observer in infinity, which means the minimum distance of the charged particles to the central object increases. A module of the tidal charge increases parabolic and hyperbolic orbits start to become unstable circular orbits, while a magnetic parameter gives the opposite effect (Fig. 1) (see e.g. our preceding research [27]). Thus the radial profile of $V_{\rm eff}$ for different values of the tidal charge Q^*, running between -0.01 and -0.03 shows that by increasing the module of Q^* from 0.01 to 0.03 we also lower the potential barrier, as compared to the Schwarzschild case, as expected for the potential of the Reissner-Nordström–type black holes.

The choice of the brane parameter's sign is stipulated according to the following reason: the negative bulk cosmological constant contributes to acceleration toward the brane, reflecting its confining role on the gravitational field. In order for U to reinforce confinement, it must be negative. An effective energy density $U = \kappa Q^*/r^4$ on the brane arising from the free gravitational field in the bulk, where κ is the positive constant, needs not be positive. Indeed, $U < 0$ is the natural case. In other words, the negative tidal charge $Q^* < 0$ is the physically more natural case. Furthermore, $Q^* < 0$ ensures that the singularity is spacelike, as in the Schwarzschild solution, whereas $Q^* > 0$ leads to a timelike singularity, which amounts to a quali-

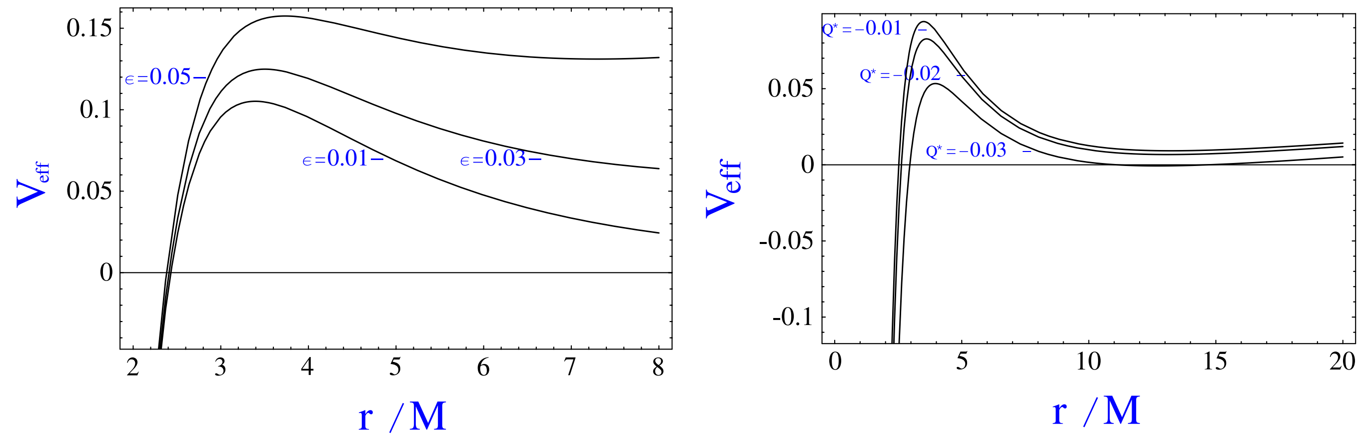

FIG. 1 (color online). Radial dependence of the effective potential of the radial motion of the charged particles around a slowly rotating black hole in a braneworld immersed in a uniform magnetic field for the different parameter of the magnetic field ϵ (left graph) and tidal charge Q^* (right graph).

tative change in the nature of the general relativistic Schwarzschild solution (see, for more details, [2]).

IV. MOTION OF TEST PARTICLE AROUND A BLACK HOLE IN A BRANEWORLD

In order to find the exact analytical solution for radius $r_{\rm ISCO}$ we assume that the external magnetic field is absent and a black hole in a braneworld is nonrotating when metric (15) can be written in the diagonal form as

$$ds^2 = -\frac{\Delta}{r^2}dt^2 + \frac{r^2}{\Delta}dr^2 + r^2 d\theta^2 + r^2 \sin^2\theta d\varphi^2, \qquad (22)$$

where $\Delta = r^2 - 2Mr + Q^*$ does not include terms being proportional to the angular momentum of a black hole. Now using the Hamilton-Jacobi method described in Sec. III one can easily find the equation of motion of the test particle in the equatorial plane of the black hole in a braneworld as

$$\frac{dt}{d\sigma} = \mathcal{E}\frac{r^2}{\Delta}, \qquad (23)$$

$$\left(\frac{dr}{d\sigma}\right)^2 = \mathcal{E}^2 - \frac{\Delta}{r^2}\left(1 + \frac{\mathcal{L}^2}{r^2}\right), \qquad (24)$$

$$\frac{d\varphi}{d\sigma} = \frac{\mathcal{L}}{r^2}. \qquad (25)$$

Using Eqs. (24) and (25) and introducing a new variable $u = 1/r$ one can obtain the following equation:

$$\left(\frac{du}{d\varphi}\right)^2 = -Q^* u^4 + 2Mu^3 - \left(1 + \frac{Q^*}{\mathcal{L}^2}\right)u^2 + \frac{2M}{\mathcal{L}^2}u - \frac{1-\mathcal{E}^2}{\mathcal{L}^2} = f(u), \qquad (26)$$

which defines the trajectory of the test particle around a black hole in a braneworld. The condition of the occurrence of circular orbits is

$$f(u) = 0, \qquad f'(u) = 0.$$

From these equations, it follows that the energy $\mathcal{E}$ and angular momentum $\mathcal{L}$ of a circular orbit of radius $r_c = u_c^{-1}$ is given by

$$\mathcal{E}^2 = \frac{(1 - 2Mu + Q^* u^2)^2}{1 - 3Mu + 2Q^* u^2}, \qquad (27)$$

$$\mathcal{L}^2 = \frac{M - Q^* u}{2Q^* u^3 - 3Mu^2 + u}. \qquad (28)$$

Figure 2 shows the radial dependence of both the energy and the angular momenta of the test particle moving on circular orbits in the equatorial plane. One can easily see that the presence of the brane parameter forces test particle to have bigger energy and angular momentum in order to be kept on its circular orbit. It is a consequence of the increase of the gravitational potential of the central object in a braneworld.

From Eqs. (27) and (28) one can easily find the minimum radius for circular orbits $r_{\rm mc}$

$$r_{\rm mc} > \frac{4Q^*}{3M - \sqrt{9M^2 - 8Q^*}}, \qquad (29)$$

or if we expand this expression in degrees of Q^*/M^2, it takes the following form:

$$r_{\rm mc} \approx 3M - \frac{2Q^*}{3M} - \frac{4Q^{*2}}{27M^3} + \mathcal{O}\left(\frac{Q^{*3}}{M^5}\right). \qquad (30)$$

In the limiting case when Q^* tends to zero $r_{\rm mc} = 3M$ which coincides with the Schwarzschild limit. The minimum radius for a stable circular orbit will occur at the point of inflexion of the function $f(u)$, or in other words, we must supplement conditions $f(u) = f'(u) = 0$ with the equation

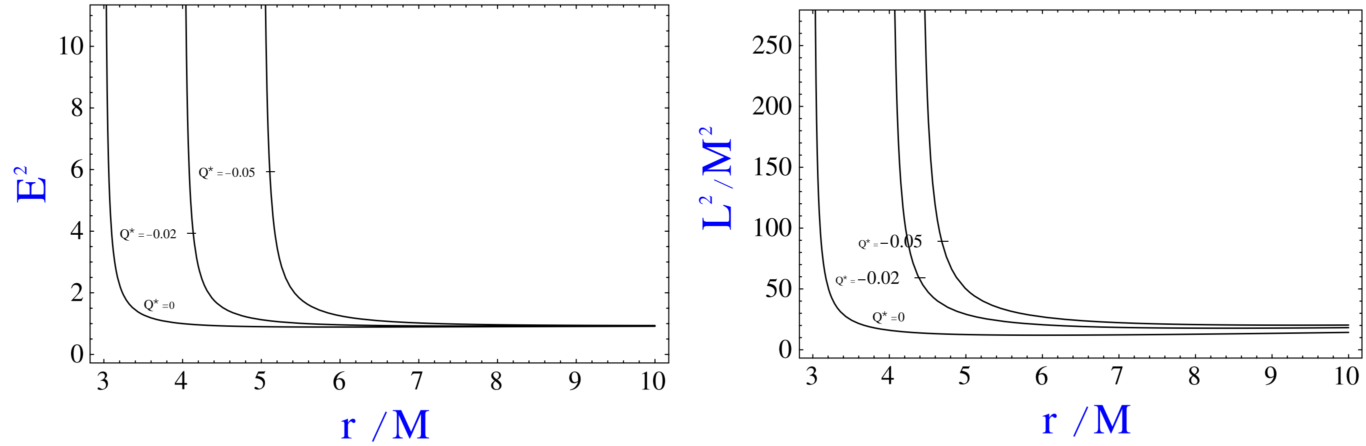

FIG. 2 (color online). Radial dependence of energy (left graph) and angular momentum (right graph) of circular orbits around a black hole in a braneworld for the different values of the brane tension Q^*. For comparison we have also plotted the Schwarzschild dependence, corresponding to $Q^* = 0$.

$f''(u) = 0$. Then one can easily obtain the equation

$$4Q^{*2}u^3 - 9MQ^*u^2 + 6M^2u - M = 0, \qquad (31)$$

and its solution in the form

$$r = \frac{4Q^*}{3M + \sqrt[3]{A - B} + \sqrt[3]{A + B}} \equiv r_{\mathrm{ISCO}}, \qquad (32)$$

where

$$A = 8MQ^* - 9M^3, \quad B = 4\sqrt{(4MQ^* - 5M^3)(MQ^* - M^3)}, \qquad (33)$$

or if we expand this expression in degrees of Q^*/M^2, it takes the following form:

$$r_{\mathrm{ISCO}} \approx 6M - 1.5\frac{Q^*}{M} + 0.0078\frac{Q^{*2}}{M^3} + \mathcal{O}\left(\frac{Q^{*3}}{M^5}\right). \qquad (34)$$

To the best of our knowledge the analytical expression (32) is the original one. It defines the limit of the stability of the innermost circular orbit in the vicinity of a black hole in a braneworld. The existence of such orbits around black holes immersed in an external magnetic field is well described in paper [23]. The critical value of the ISCO radii is $r_{\mathrm{ISCO}} = 6M$, which corresponds to the ISCO of a spinless test particle in the Schwarzschild spacetime.

After discussing the effective potential of the radial motion of test particles around a black hole immersed in the external magnetic field, the authors of paper [23] concluded that the minimum value of the test particle angular momentum corresponds to the orbit with the innermost stable circular radius. Numerical solutions with similar results for r_{ISCO} around a rotating black hole in a braneworld and circular orbits in accretion disks have been studied in papers [13,20], respectively.

The dependence of the minimum radius for circular orbits r_{mc} and radius of ISCO around a black hole from the brane tidal charge is plotted in Fig. 3, where the values related to the Schwarzschild black hole correspond to $Q^* = 0$. One can easily see from the plots that the presence of the tidal charge forces the radius of the stable orbits to be shifted away from the central object in the direction of an observer at infinity which confirms the earlier results of Aliev and Gümrükçüoğlu [20].

The variation of Q^* also modifies the position of the marginally stable orbit, as shown by the shift of the ISCO, which is presented in the left plot in the Fig. 3. The negative decreasing charges lead to the increase of ISCO radius. By decreasing the value of Q^* from 0 to -5, we shift the radius of ISCO to bigger and bigger values. The lower values of the potential for Q^* involve a lower specific energy of the orbiting particles. As we decrease Q^* from 0 to -5, ISCO radius is increasing from values greater than the radius of the marginally stable orbit for the Schwarzschild geometry to bigger ones. The efficiency has an opposite trend with compare to angular momentum: for negative tidal charges it has bigger values than in the case of the Schwarzschild black holes.

Next, we will give a clear derivation of the capture cross section of slowly moving test particles a hole in a braneworld. (Slow motion means that $\mathcal{E} \simeq 1$ at the infinity.) The critical value of the particle's angular momentum, $\mathcal{L}_{\mathrm{cr}}$, hinges upon the existence of a multipole root of the polynomial $f(u)$ in (26) [30]. For convenience hereafter we rewrite Eq. (26) in terms of dimensionless parameters as radial coordinate $r \to r/M$, momentum $\mathcal{L} \to \mathcal{L}/M$, and tidal charge $Q^* \to Q^*/M^2$:

$$r^3 - \frac{\mathcal{L}^2 + Q^*}{2}r^2 + \mathcal{L}^2 r - \frac{Q^*\mathcal{L}^2}{2} = 0. \qquad (35)$$

The cubic equation (35) has a multiple root if and only if its discriminant vanishes. After simple algebraic transformations one can easily obtain the following equation for a particle angular momentum:

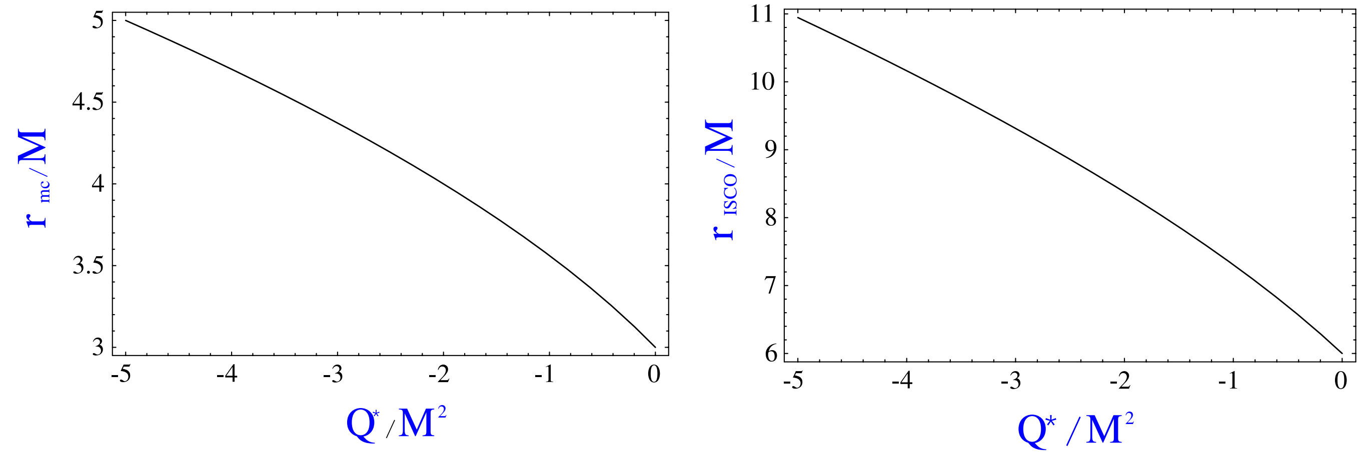

FIG. 3 (color online). Dependence of the lower limit for the radii of circular orbits r_{mc} (left graph) and ISCO r_{ISCO} (right graph) from the tidal charge Q^*.

$$\mathcal{L}^6(1 - Q^*) - \mathcal{L}^4(3Q^{*2} - 20Q^* + 16) - \mathcal{L}^2 Q^{*2}(8 + 3Q^*) - Q^{*4} = 0, \tag{36}$$

which has an exact solution in the form

$$\mathcal{L}_{\rm cr}^2 = \begin{cases} \sqrt[3]{-B_1/2 + \sqrt{D}} + \sqrt[3]{-B_1/2 - \sqrt{D}} - \frac{(20Q^* - 3Q^{*2} - 16)^2}{3(1-Q^*)}, & D \geq 0; \\ 2\sqrt{\frac{-A_1}{3}}\cos\{\frac{1}{3}\arccos[-B_1/(2\sqrt{-(A_1/3)^2})]\} - \frac{(20Q^* - 3Q^{*2} - 16)^2}{3(1-Q^*)}, & D < 0. \end{cases} \tag{37}$$

Here we have introduced the following notations:

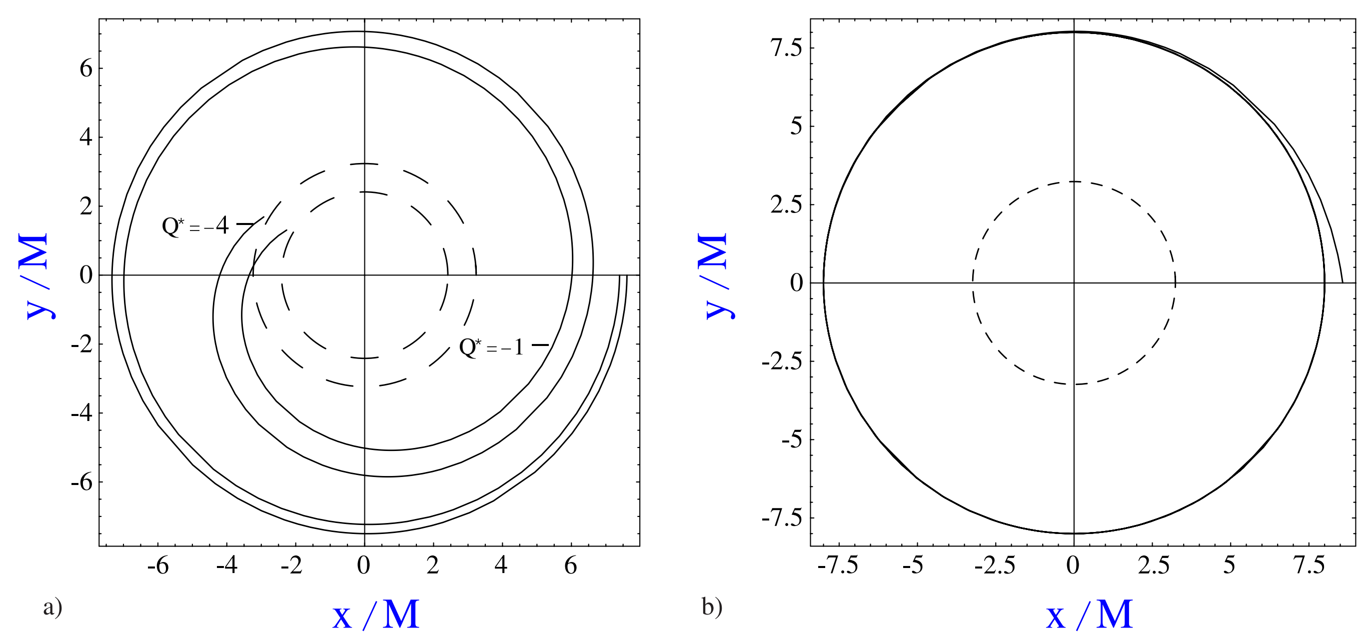

FIG. 4 (color online). (a). Orbits of the test particle falling into a central black hole for different values of the tidal charge Q^*. (b). Stable circular orbit of the test particle around a black hole in a braneworld. In all plots horizons are shown with dashed lines.

$$A_1 = -\frac{(20Q^* - 3Q^{*2} - 16)^2}{3(1-Q^*)^2} - \frac{8Q^{*2} + 3Q^{*3}}{1-Q^*},$$
$$B_1 = 2\frac{(20Q^* - 3Q^{*2} - 16)^2}{27(1-Q^*)^3} - \frac{(20Q^* - 3Q^{*2} - 16)^2(8Q^{*2} + 3Q^{*3})}{1-Q^*} - \frac{Q^{*4}}{1-Q^*},$$
$$D = \frac{A_1^3}{27} + \frac{B_1^2}{4}.$$

In the limiting case, i.e. when the tidal charge vanishes the solution of Eq. (36) is $\mathcal{L} = 4$, which coincides with the critical angular momentum for the particle capture cross section for a Schwarzschild black hole [31]. As a particle with a critical angular momentum travels from infinity toward the black hole in a braneworld, it spirals into an unstable circular orbit of radius given as

$$r_{\mathrm{uc}} = 2\sqrt[3]{\left(\frac{\mathcal{L}^2 + Q^*}{6}\right)^3 - \mathcal{L}\left(\frac{\mathcal{L}^2 + Q^*}{6}\right) + \mathcal{L}^2 Q^*} + \frac{\mathcal{L}^2 + Q^*}{6}. \tag{38}$$

Finally in Fig. 4 we present the shapes of different kinds of trajectories of test particles around a black hole in a braneworld, which are given by Eq. (26). The trajectories of test particles falling to the central black hole in a braneworld for different values of the brane parameter are shown in Fig. 4(a). From the plot one can obtain that increase of the module of the brane parameter causes orbits to shift to an observer at the infinity, which is a consequence of an increase of the radius of the event horizon by braneworld effects. Figure 4(a) illustrates the sample of unstable circular orbits of the particles, while Fig. 4(b)) shows the shape of the circular orbits around a black hole in the braneworld.

V. CONCLUSION

We have concentrated here on the basic physical properties of particle motion and a magnetic field in the background spacetime metric of the braneworld black holes. The motivation for this research is caused by the fact that testing strong field gravity and the detection of the possible deviations from standard general relativity, signaling the presence of new physics, remains one of the most important objectives of observational astrophysics. Because of their compact nature, black holes provide an ideal environment to perform precise relativistic measurements, in particular, the observational possibilities for testing the DMPR solution of the vacuum field equations in brane world models.

Here the physical parameters of the effective potential and ISCO have been explicitly obtained for several values of the parameters characterizing the vacuum DMPR solution of the field equations in the braneworld models. We have found the original exact expression for the lower limit of the innermost stable circular orbits of the test particle around a black hole in a braneworld. (Before ISCO, behavior in braneworld models was investigated only numerically [13,20].) Then we have plotted the dependence of the ISCO radius from the brane tidal charge and particle trajectories around a black hole in a braneworld.

The best constraints on the braneworld black hole parameters were recently obtained from the classical tests of general relativity (perihelion precession, deflection of light, and the radar echo delay, respectively) [11]. The existing observational solar system data on the perihelion shift of Mercury, on the light bending around the Sun (obtained using long-baseline radio interferometry), and ranging to Mars using the Viking lander, were applied to the relativistic effects in DMPR spacetime, constrained the numerical values of the brane parameter. The strongest limit $|Q^*| \lesssim 10^8\ \mathrm{cm}^2$ was obtained from Mercury's perihelion precession.

The recent measurements of the ISCO radius in accretion disks around black holes may also give alternate constraints on the numerical values of the brane tidal charge. All the astrophysical quantities related to the observable properties of the accretion disk can be obtained from the black hole metric and observations in the near infrared or x-ray bands have provided important information about the spin of the black holes [32–34]. It was stated that rotating black holes have spins in the range $0.5 \lesssim a \lesssim 1$, that is, according to the observations ISCO radii are essentially shifted towards the central objects and there is not any effect measured from the brane tidal charge which acts in the opposite direction.

Because of the differences in the spacetime structure, the braneworld black holes present some important differences with respect to their disc accretion properties, as compared to the standard general relativistic Schwarzschild and Kerr cases. Therefore, the study of the innermost stable orbits in the vicinity of compact objects is a powerful indicator of their physical nature. Since the ISCO radius in the case of the braneworld black holes is different compared to the standard general relativistic case, the astrophysical determination of these physical quantities could discriminate, at least in principle, between the different gravity theories, and give some constrains on the existence of the extra dimensions. Finally, since there was no braneworld effect on stable orbits around black holes on the scale of the rotational parameter a order of $10^8\ \mathrm{cm}^2$, we may conclude that from an astrophysical point of view on the basis of a comparison of observations of ISCO in accretion disks around black holes and ISCO analysis around a black hole in a braneworld that the brane tidal charge has an upper limit $\lesssim 10^9\ \mathrm{cm}^2$. We roughly estimated that one order less magnitude of Q^* may not affect the observational data on ISCO data around black holes.

ACKNOWLEDGMENTS

The authors gratefully thank Naresh Dadhich for his invaluable help, extensive discussions, and for editing the text and making important corrections and comments. They also thank Valeria Kagramanova for useful discussions. The authors thank the IUCAA for warm hospitality during their stay in Pune and AS-ICTP for the travel support through the BIPTUN program. This research is supported in part by Projects No. FA-F2-079 and No. FA-F2-F061 of the UzAS. B. J. A acknowledges partial financial support from the DAAD and the IAU C46-PG-EA programs. This work is partially supported by the ICTP through the OEA-PRJ-29 project and the Regular Associateship grant.

[1] L. Randall and R. Sundrum, Phys. Rev. Lett. **83**, 3370 (1999).
[2] N. K. Dadhich, R. Maartens, P. Papodopoulos, and V. Rezania, Phys. Lett. B **487**, 1 (2000).
[3] R. Maartens, Living Rev. Relativity **7**, 7 (2004), http://www.livingreviews.org/lrr-2004-7.
[4] C. R. Keeton and A. O. Petters, Phys. Rev. D **73**, 104032 (2006).
[5] C. R. Keeton and A. O. Petters, Phys. Rev. D **72**, 104006 (2005); **73**, 044024 (2006).
[6] V. Bozza, Phys. Rev. D **66**, 103001 (2002).
[7] E. F. Eiroa, Phys. Rev. D **71**, 083010 (2005).
[8] R. Whisker, Phys. Rev. D **71**, 064004 (2005).
[9] S. Pal and S. Kar, Classical Quantum Gravity **25**, 045003 (2008).
[10] L. Iorio, Classical Quantum Gravity **22**, 5271 (2005).
[11] C. G. Böhmer, T. Harko, and F. S. N. Lobo, Classical Quantum Gravity **25**, 045015 (2008).
[12] A. Kotrlová, Z. Stuchlik, and G. Török, Classical Quantum Gravity **25**, 225016 (2008).
[13] C. S. J. Pun, Z. Kovács, and T. Harko, Phys. Rev. D **78**, 084015 (2008).
[14] E. Hackmann, V. Kagramanova, J. Kunz, and C. Lämmerzahl, Phys. Rev. D **78**, 124018 (2008).
[15] L. Á. Gergely and B. Darázs, Publications of the Astronomy Department of the Eotvos University **17**, 213 (2006).
[16] L. Á. Gergely, Z. Keresztes, and M. Dwornik, Classical Quantum Gravity **26**, 145002 (2009).
[17] J. Schee and Z. Stuchlík, Gen. Relativ. Gravit. **41**, 1795 (2009).
[18] Z. Stuchlík and A. Kotrlová, Gen. Relativ. Gravit. **41**, 1305 (2009).
[19] J. Schee and Z. Stuchlík, Int. J. Mod. Phys. D **18**, 983 (2009).
[20] A. N. Aliev and A. E. Gümrükçüoğlu, Phys. Rev. D **71**, 104027 (2005).
[21] R. da Rocha and C. H. Coimbra-Araujo, Proc. Sci., IC2006 (2006) 065.
[22] B. J. Ahmedov and F. J. Fattoyev, Phys. Rev. D **78**, 047501 (2008).
[23] R. A. Konoplya, Phys. Rev. D **74**, 124015 (2006).
[24] R. A. Konoplya, Phys. Lett. B **644**, 219 (2007).
[25] A. N. Aliev and A. E. Gümrükçüoğlu, Classical Quantum Gravity **21**, 5081 (2004).
[26] R. M. Wald, Phys. Rev. D **10**, 1680 (1974).
[27] A. A. Abdujabbarov, B. J. Ahmedov, and V. G. Kagramanova, Gen. Relativ. Gravit. **40**, 2515 (2008).
[28] A. N. Aliev and V. P. Frolov, Phys. Rev. D **69**, 084022 (2004).
[29] N. Dadhich and Z. Ya. Turakulov, Classical Quantum Gravity **19**, 2765 (2002).
[30] A. F. Zakharov, Classical Quantum Gravity **11**, 1027 (1994).
[31] C. W. Misner, K. S. Thorne, and J. A. Wheeler, *Gravitation* (Freeman, San Francisco, 1973).
[32] R. Shafee, J. E. McClintock, R. Narayan, S. W. Davis, L.-X. Li, and R. A. Remillard, Astrophys. J. **636**, L113 (2006).
[33] R. Shafee, R. Narayan, and J. E. McClintock, Astrophys. J. **676**, 549 (2008).
[34] J. F. Steiner, J. E. McClintock, R. A. Remillard, R. Narayan, and L. Gou, arXiv:0907.2920v1.